Supporting information

Two-step assembly induced Fe^0-anchored graphitic N-rich graphene with biactive centers for enhanced heterogeneous peroxymonosulfate activation

Junjie Zhang [a], Wenran Gao [b], Yamei Yue [a], Wei Wang [a, *], Fatang Tan [a], Xinyun Wang [a], Xueliang Qiao [a], Po Keung Wong [c]

[a] State Key Laboratory of Materials Processing and Die & Mould Technology, School of Materials Science and Engineering, Huazhong University of Science and Technology, Wuhan 430074, Hubei, China

[b] Lab of Biomass Energy and Functional Carbon Materials, College of Materials Science and Engineering, Nanjing Forestry University, Nanjing, 210018, Jiangsu, China

[c] School of Life Sciences, The Chinese University of Hong Kong, Shatin, NT, Hong Kong SAR, China

* Corresponding author

Wei Wang, Tel/fax: +86-27-87541540, E-mail: weiwang@hust.edu.cn

Text S1-S4

Figs. S1-S27

Table S1-S9

Text S1: Measurement of Fe contents in Fe-GNG samples

The Fe contents in Fe-GNG samples were measured by using an inductively coupled plasma mass spectrometer (ICP, ELAN DRC-e, PerkinElmer). Specifically, 30 mg Fe-GNG was refluxed in 50 mL concentrated HNO_3 for 5 h to completely dissolve iron species. The dispersion solution was filtered and washed several times by water. The obtained filtrate was collected and transferred into a 250 mL volumetric flask, and added water to 250 mL. Then, the iron contents in the above solutions were detected by ICP. The iron concentrations in solutions were determined to be 0.82, 0.78 and 0.72 mg/L for Fe-GNG1, Fe-GNG2 and Fe-GNG3, respectively. Thus, the Fe contents for Fe-GNG1, Fe-GNG2 and Fe-GNG3 were calculated to be 54.67, 52.00 and 48.00 wt%, respectively.

Text S2: Contribution of leaching Fe to RhB degradation

In order to study the contribution of leaching Fe to RhB degradation, the following experiments were conducted. 5 mg of Fe-GNG2 was added into a 500 mL beaker with 200 mL of 20 mg/L RhB and the solution pH was adjusted to 2.2, 4.0, 6.8, 8.3 and 10.3, respectively. After stirring for 70 min, the catalyst was magnetic separated and the solution was collected. Then, 12 mg of PMS was added into the solution to explore the degradation of RhB by leaching Fe from Fe-GNG2 at 70 min.

Text S3: DFT Calculations

Based on our previous work [1], density functional theory (DFT) was employed to calculate the adsorption energy of PMS on different N sites in graphene. A $C_{42}H_{16}$ model was used as the framework for pristine graphene. Vienna ab-initio simulation package (VASP)

was used to conduct calculations with the perdew-burke-ernzerhof (PBE) exchange correlation functional [2]. DFT-D3 method was utilized to describe van der Waals interactions [3]. The cut off energy was 400 eV and the interactions between the atomic cores and electrons were described by the projector augmented wave (PAW) method [4]. All structures were optimized until the force on each atom was less than 0.02 eV/Å. The sizes of unit cell for pristine graphene, pyrrolic N, pyridinic N, and graphitic N doped graphene were 25 × 25 × 15 Å. The Brillouin zone was only sampled by gamma point. The adsorption energies (E_{ads}) of PMS on different N sites were calculated by the following equation: $E_{ads} = E^*_{SO3OH} - E_{graphene} - E_{SO3OH}$, where E^*_{SO3OH}, $E_{graphene}$ and E_{SO3OH} were the energies of graphene with adsorbed PMS, graphene alone and free PMS molecule, respectively.

Text S4: Measurement of electrochemical impedance spectroscopy (EIS)

Electrochemical impedance spectroscopy was measured on a CS350 electrochemical analyzer (CorrTest, China) by using a single-compartment three-electrode glass cell at room temperature. The counter electrode was a platinum foil and the reference electrode was a saturated calomel electrode. The working electrodes were fabricated by blade-coating of slurry on a FTO glass and dried in air before use. The slurry was prepared by mixing 0.1 g of obtained materials and 0.03 g polyethylene glycol (PEG, molecular weight: 20,000) in 0.5 mL water. 0.1 M Na_2SO_4 aqueous solution was employed as the electrolyte solution for the EIS measurements. Impedance was measured at open circuit potential with the frequency ranging from 0.1 Hz to 10 kHz and an AC voltage magnitude of 5 mV.

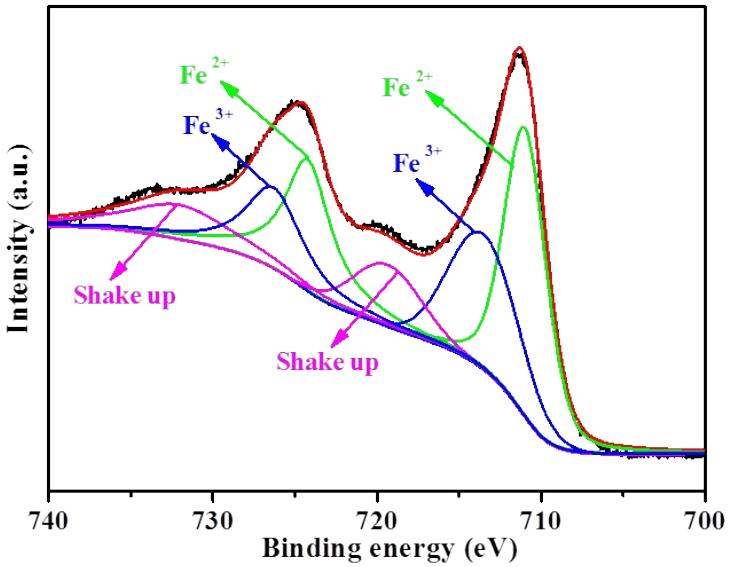

Fig. S1. High-resolution Fe 2p XPS spectrum of GO@MC-Fe sample.

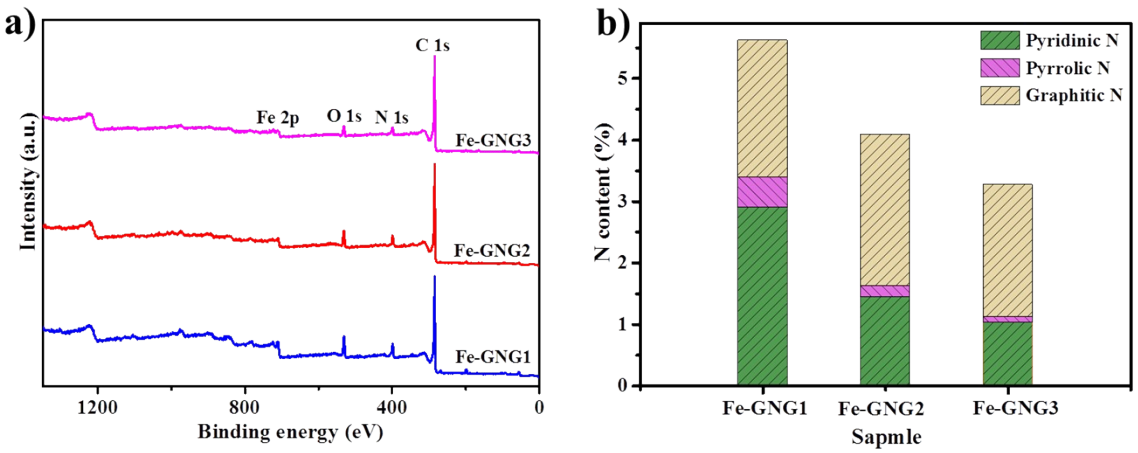

Fig. S2. a) XPS survey spectra of Fe-GNG samples. b) Contents of three nitrogen species in Fe-GNG samples.

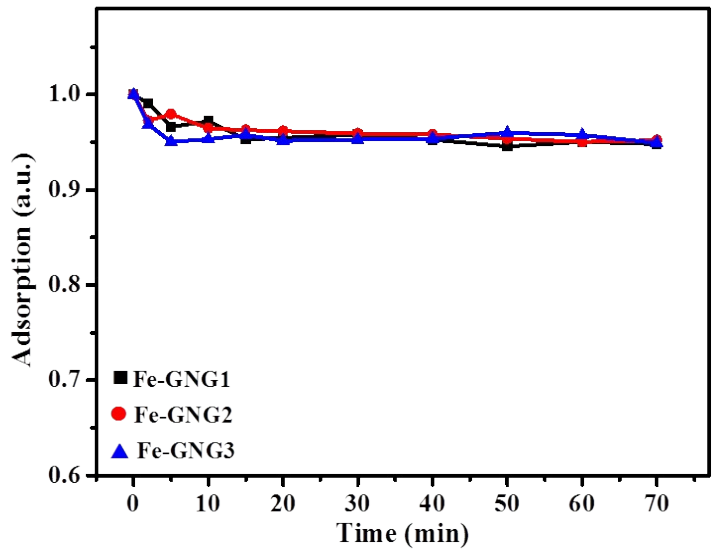

Fig. S3. Adsorption performance of Fe-GNG samples (Condition: [RhB] = 20 mg/L, [Fe-GNG] = 25 mg/L).

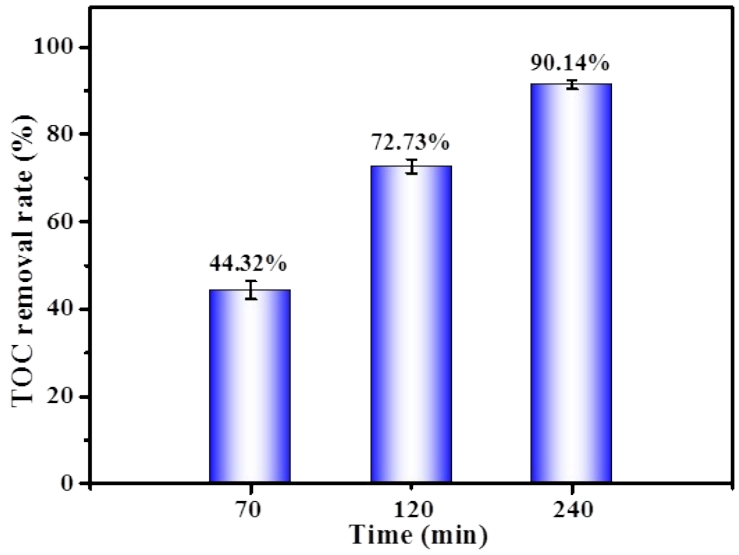

Fig. S4. TOC removal rate of RhB in Fe-GNG2/PMS system (Condition: [PMS] = 0.10 mM, [RhB] = 20 mg/L, [Fe-GNG2] = 25 mg/L).

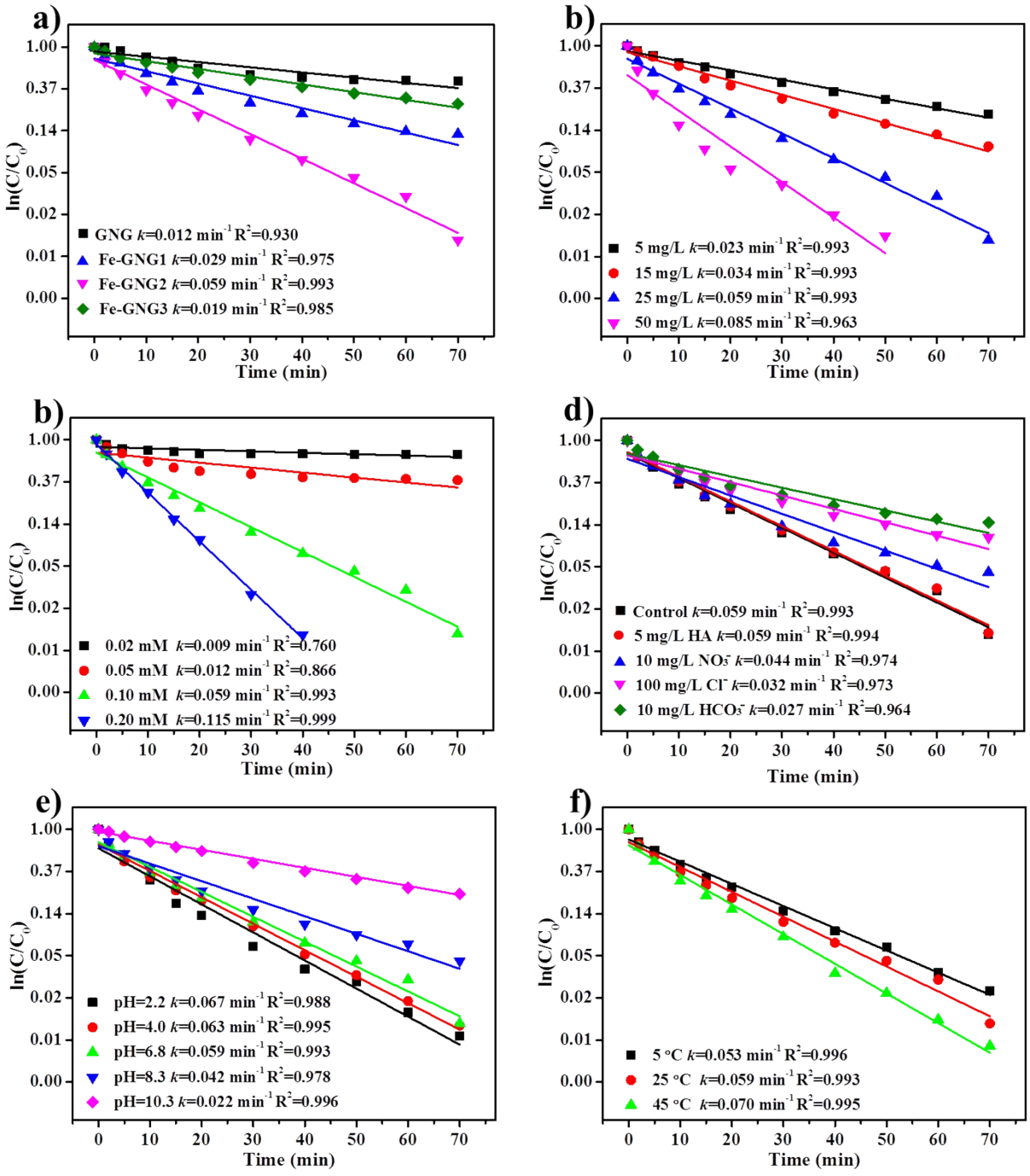

Fig. S5. a) First-order kinetic curves of RhB degradation under different samples. (Condition: [PMS] = 0.10 mM, [RhB] = 20 mg/L, [Fe-GNG] = 25 mg/L). First-order kinetic curves of RhB degradation under different conditions: b) Fe-GNG2 dosage, c) PMS dosage, d) common matrix species, e) initial solution pH and f) degradation temperature.

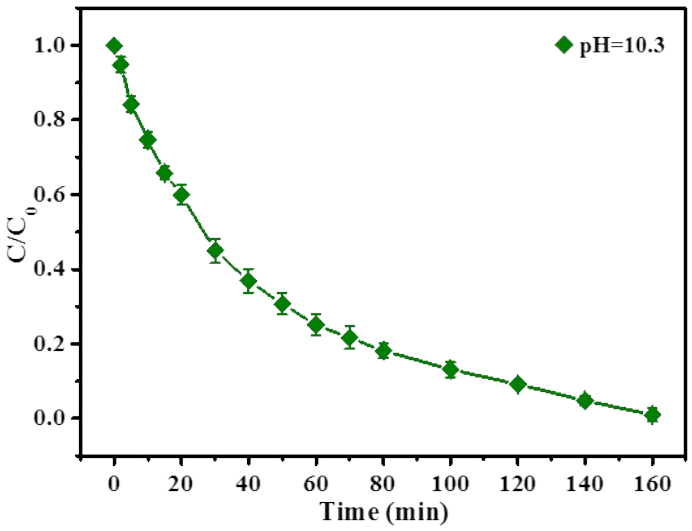

Fig. S6. Catalytic performance of Fe-GNG2 for RhB degradation at pH 10.3 (Condition: [PMS] = 0.10 mM, [RhB] = 20 mg/L, [Fe-GNG2] = 25 mg/L).

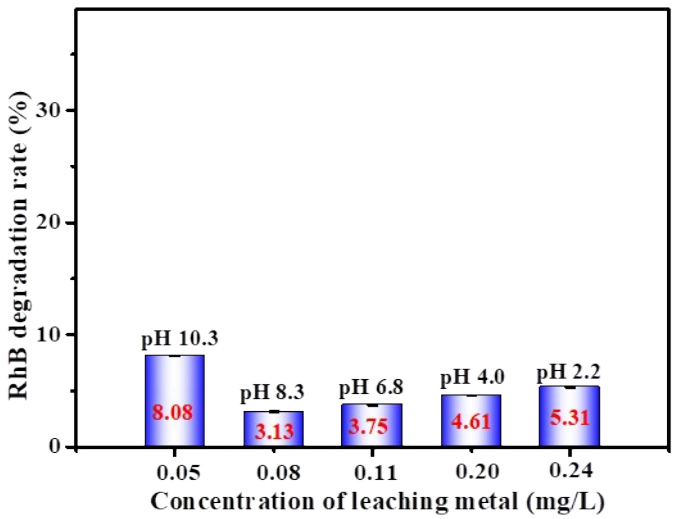

Fig. S7. Contribution of leaching metal to RhB removal.

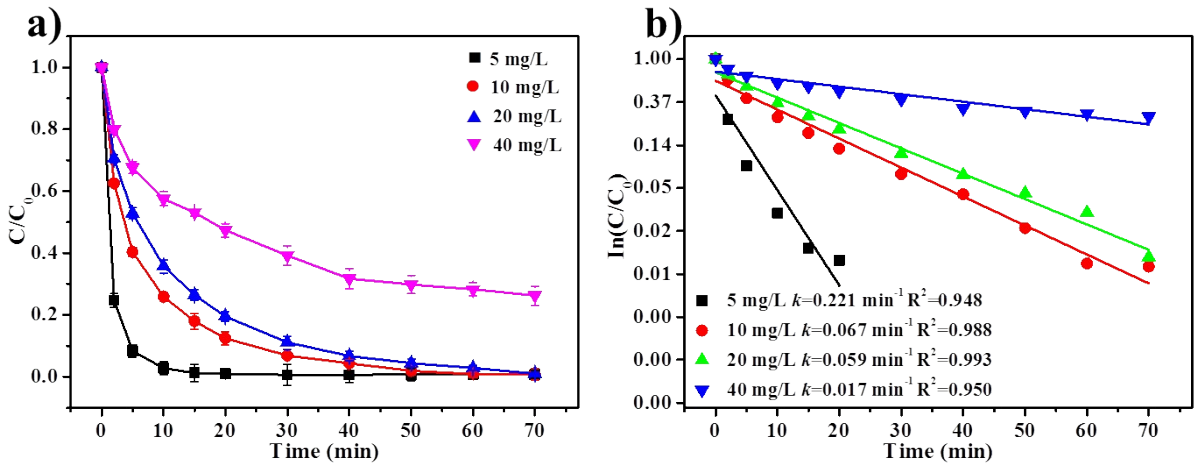

Fig. S8. a) Effect of initial RhB concentration on RhB removal and corresponding b) first-order kinetic curves (Condition: [PMS] = 0.10 mM and [Fe-GNG] = 25 mg/L).

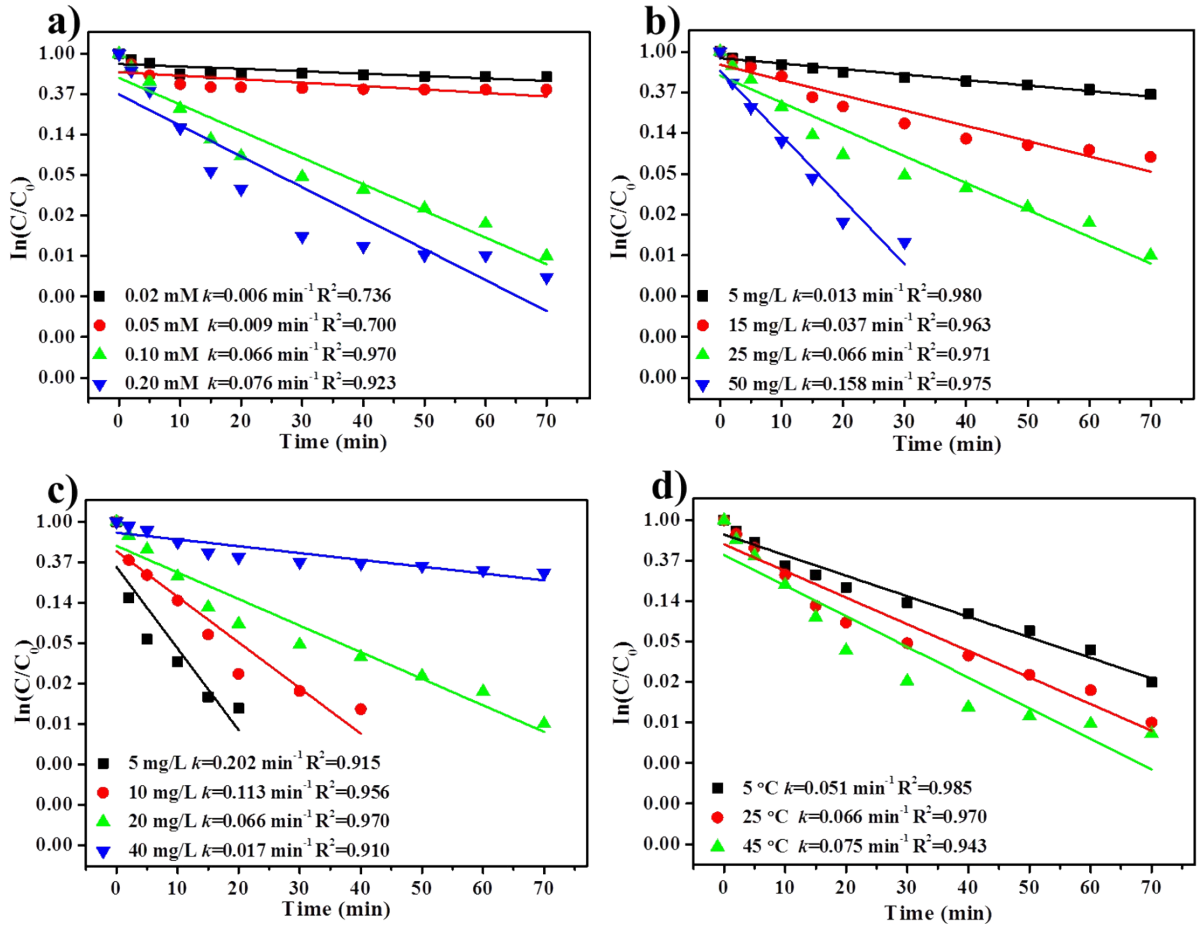

Fig. S9. First-order kinetic curves of CTC degradation at varying a) PMS dosage, b) Fe-GNG2 dosage, c) initial CTC concentration and d) degradation temperature.

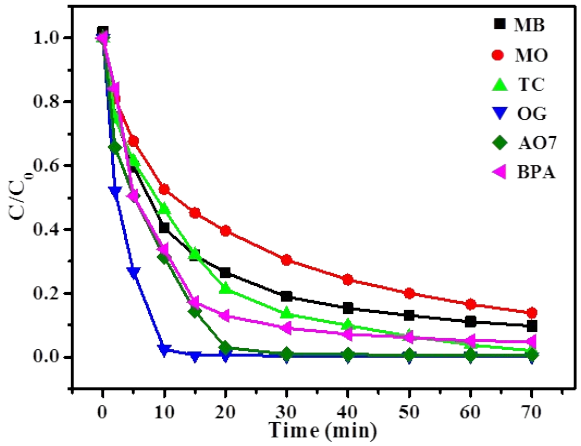

Fig. S10. Degradation of other organic pollutants in FeGNG2/PMS system (Condition: [PMS] = 0.10 mM, [pollutant] = 20 mg/L, [Fe-GNG2] = 25 mg/L).

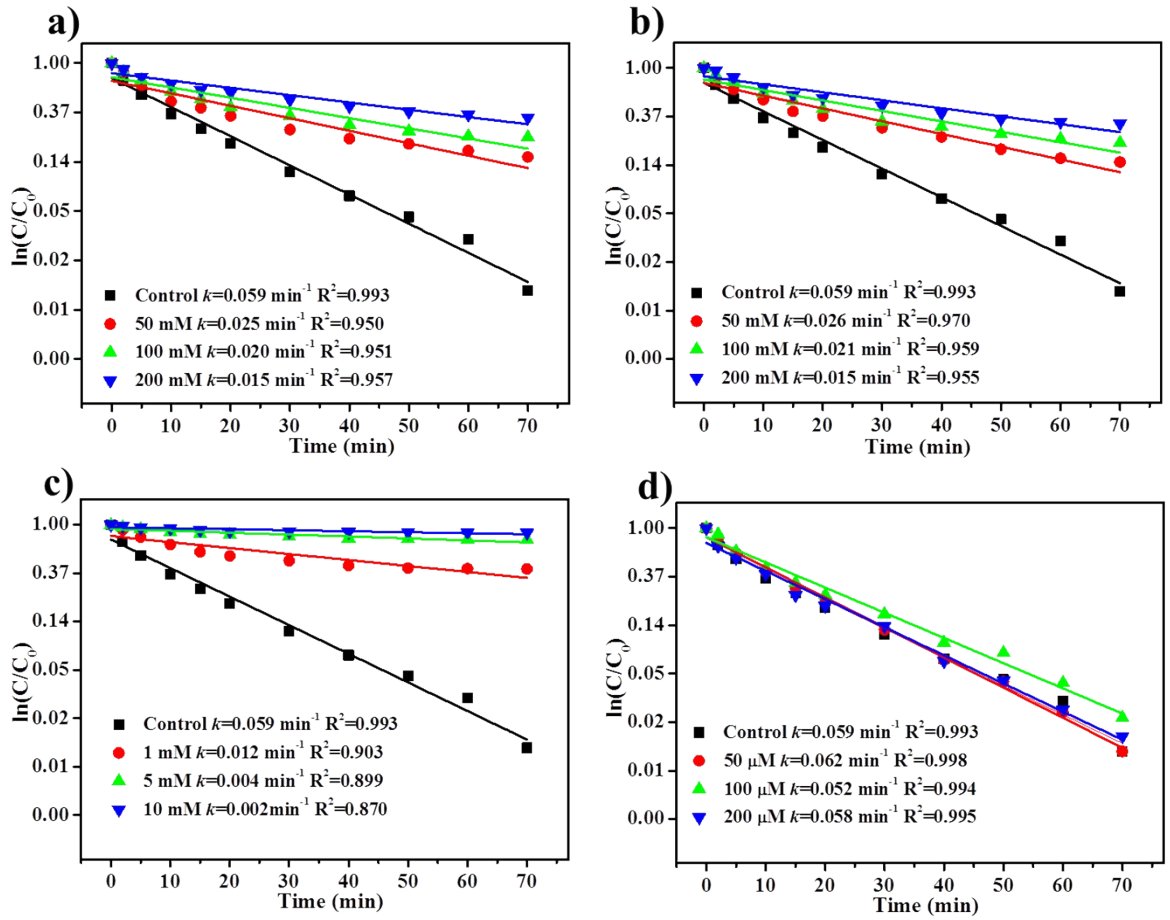

Fig. S11. First-order kinetic curves of RhB degradation in different scavenger systems: a) EtOH, b) IPA, c) FFA and d) *p*BZQ (Condition: [PMS] = 0.10 mM, [RhB] = 20 mg/L, [Fe-GNG] = 25 mg/L).

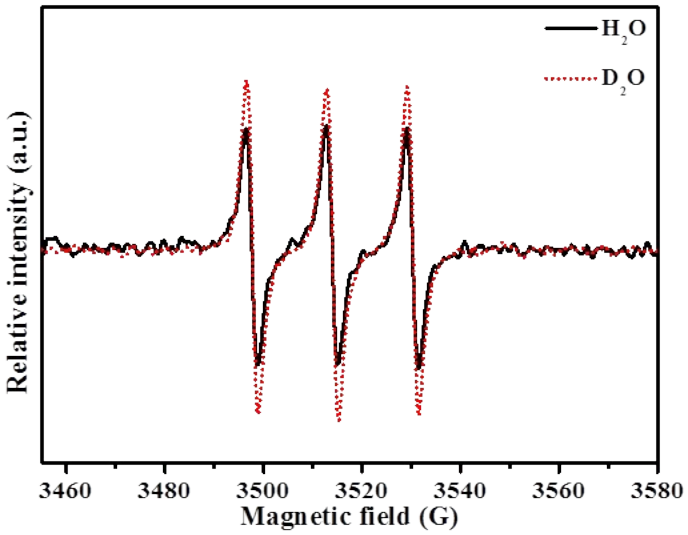

Fig. S12. EPR spectra of TEMP-$^1O_2$ in H_2O and D_2O.

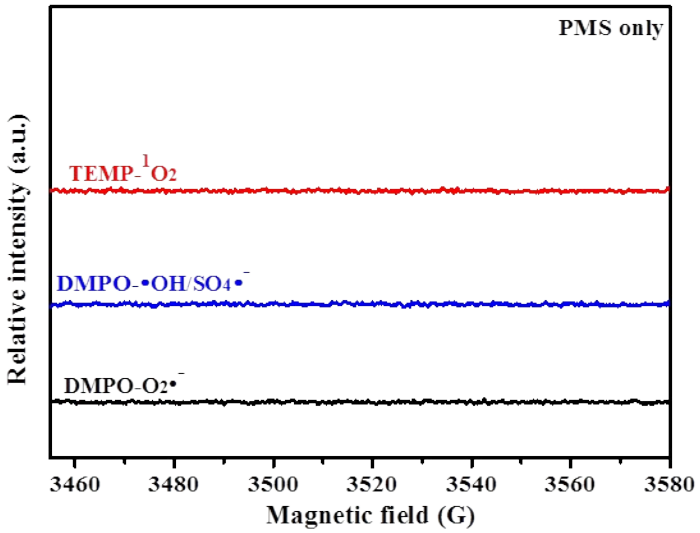

Fig. S13. EPR spectra of DMPO-O_2•$^-$, DMPO-•OH/SO_4•$^-$ and TEMP-$^1O_2$ in single PMS system.

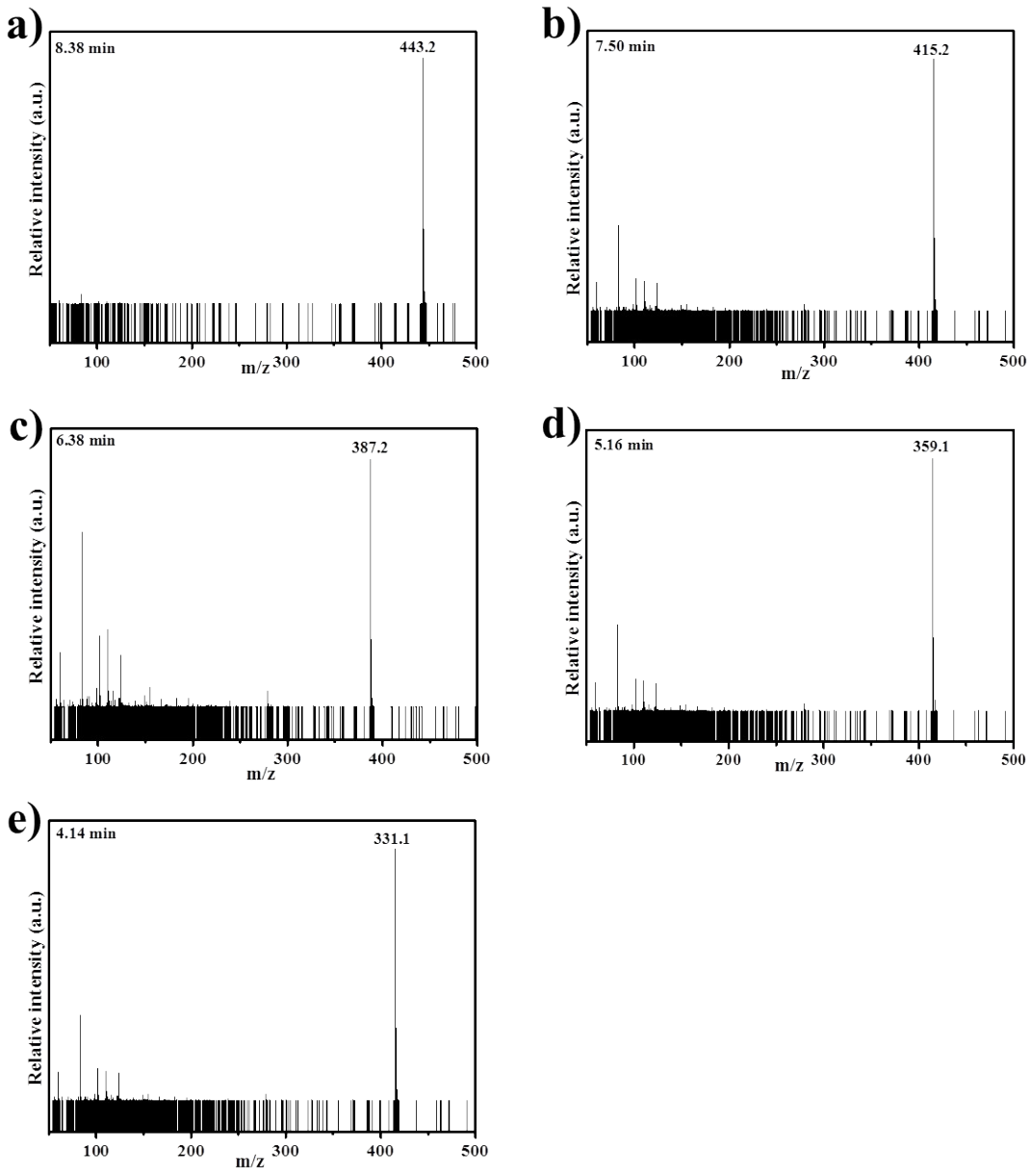

Fig. S14. LC-MS spectra of N-de-ethylation products in Fe-GNG2/PMS system.

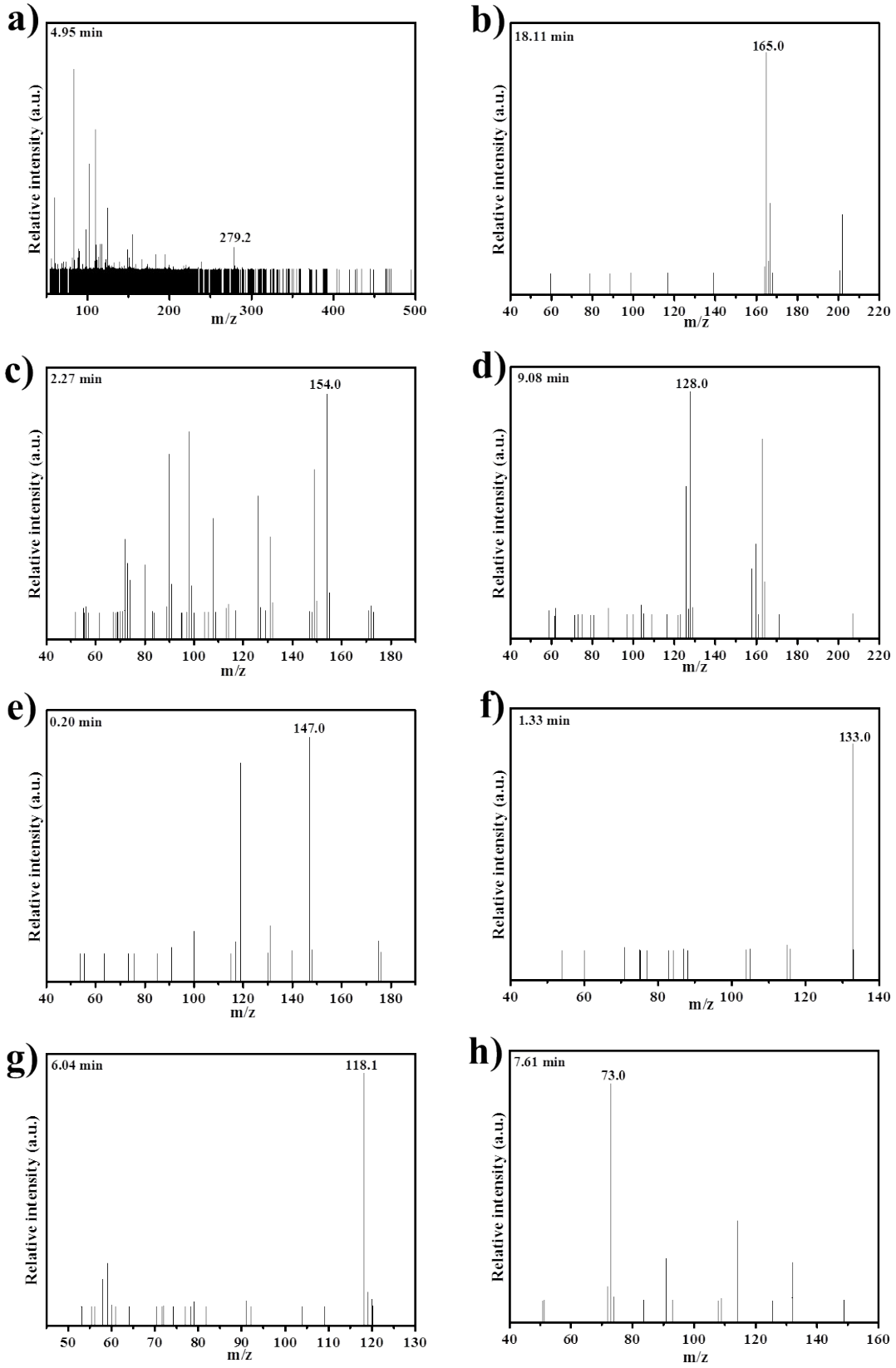

Fig. S15. LC-MS spectra of RhB degradation products via radical pathway in Fe-GNG2/PMS system.

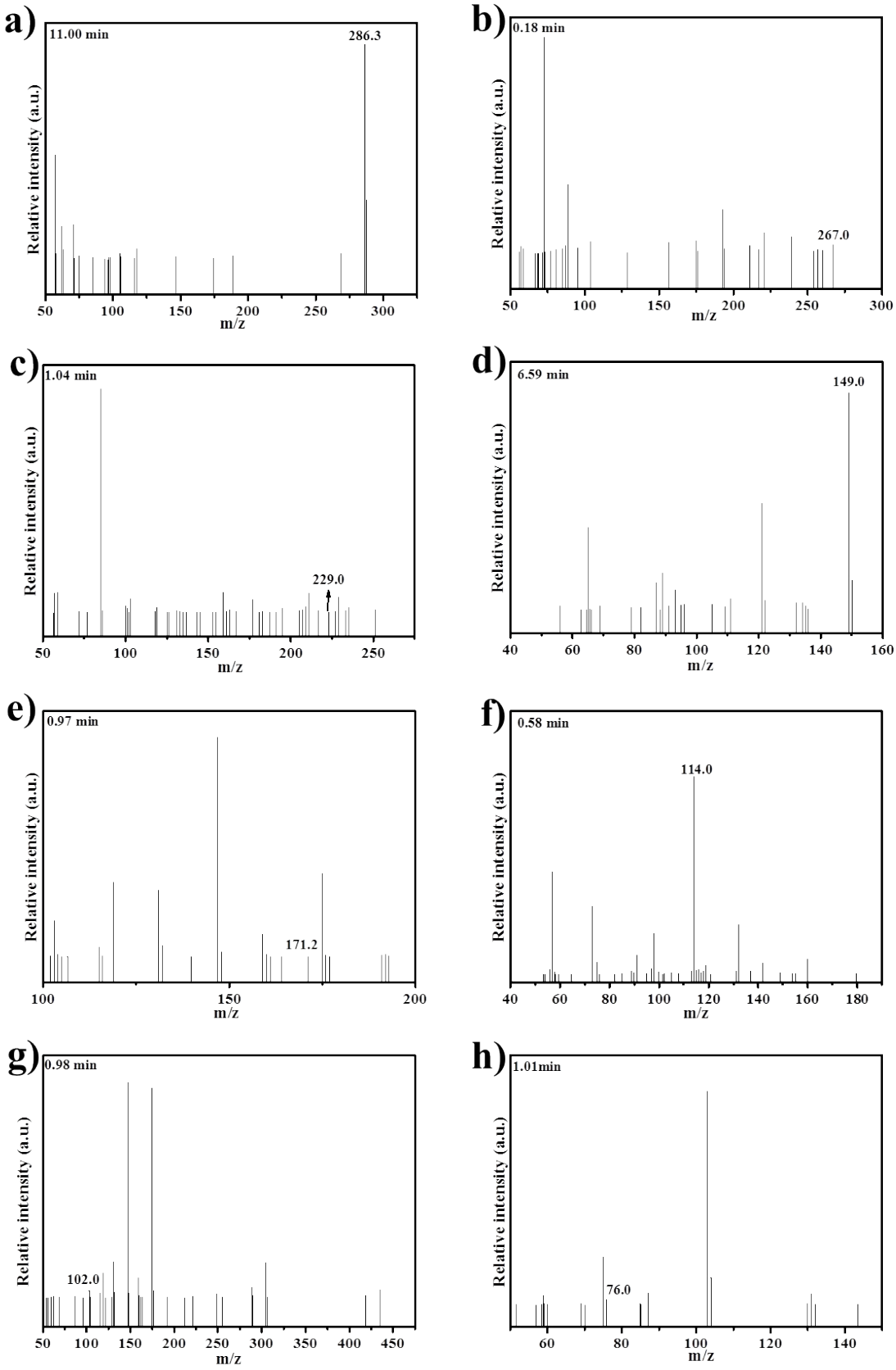

Fig. S16. LC-MS spectra of RhB degradation products via nonradical pathway in Fe-GNG2/PMS system.

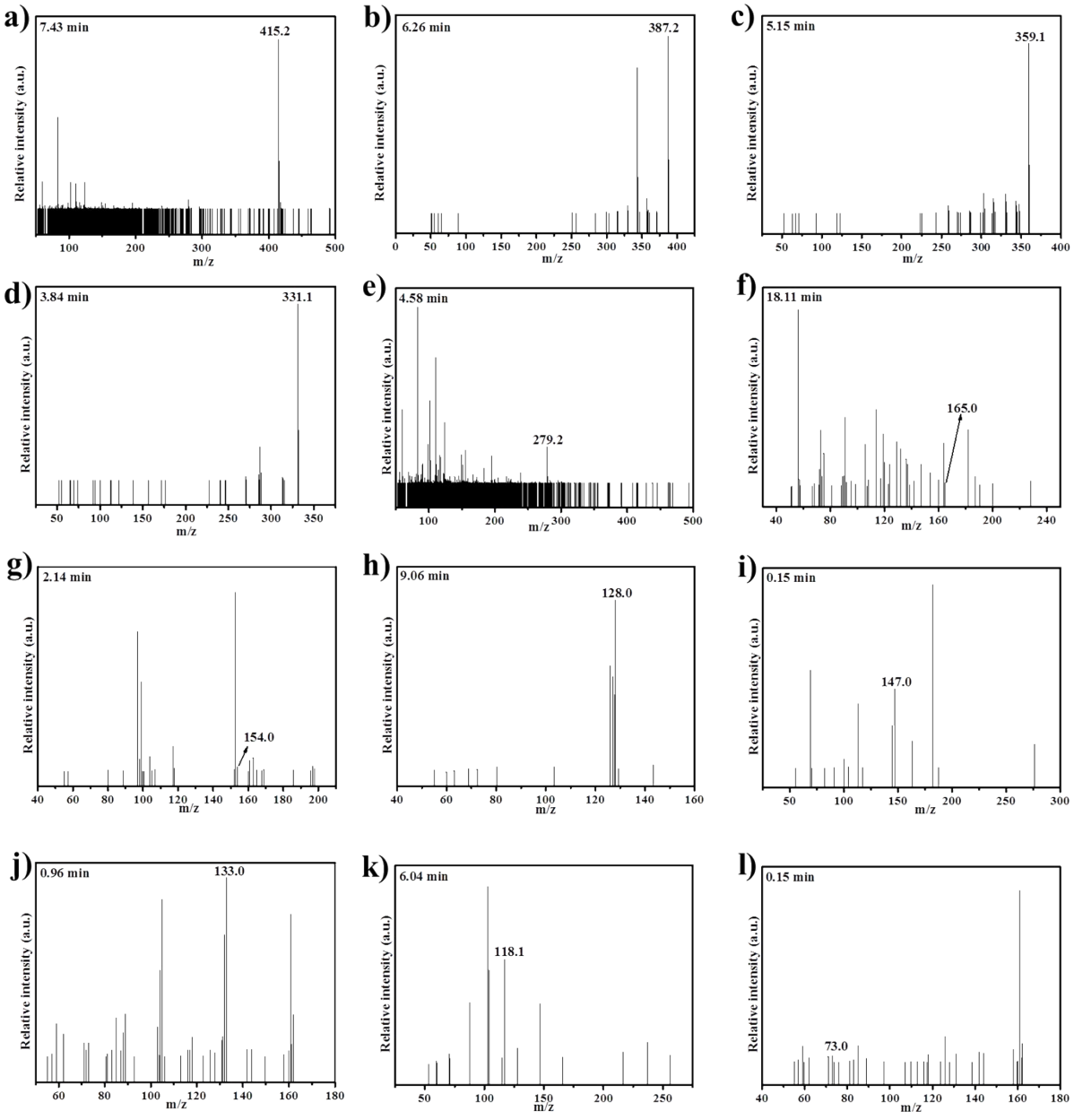

Fig. S17. LC-MS spectra of RhB degradation products in Fe^0/PMS system.

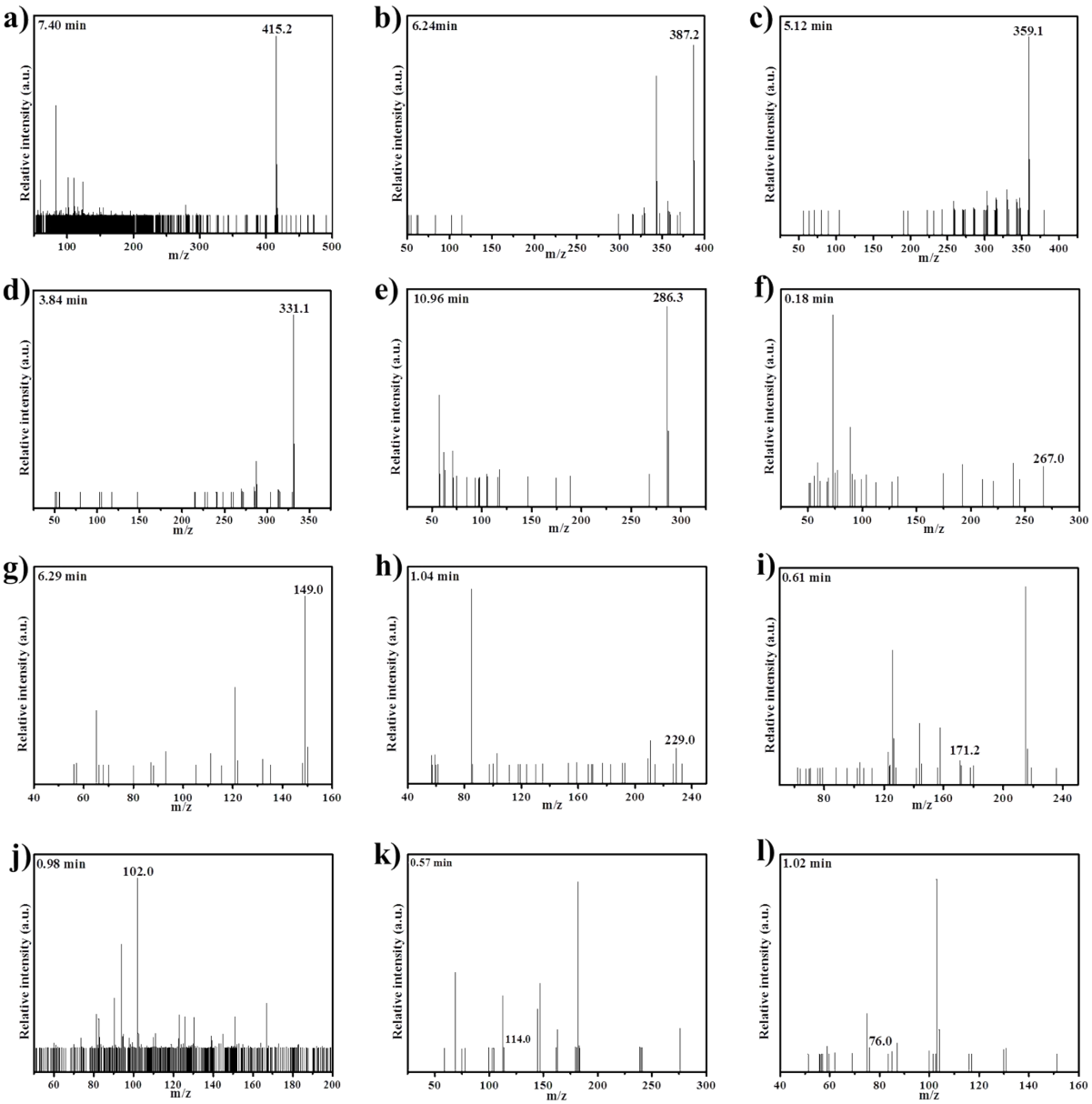

Fig. S18. LC-MS spectra of RhB degradation products in GNG/PMS system.

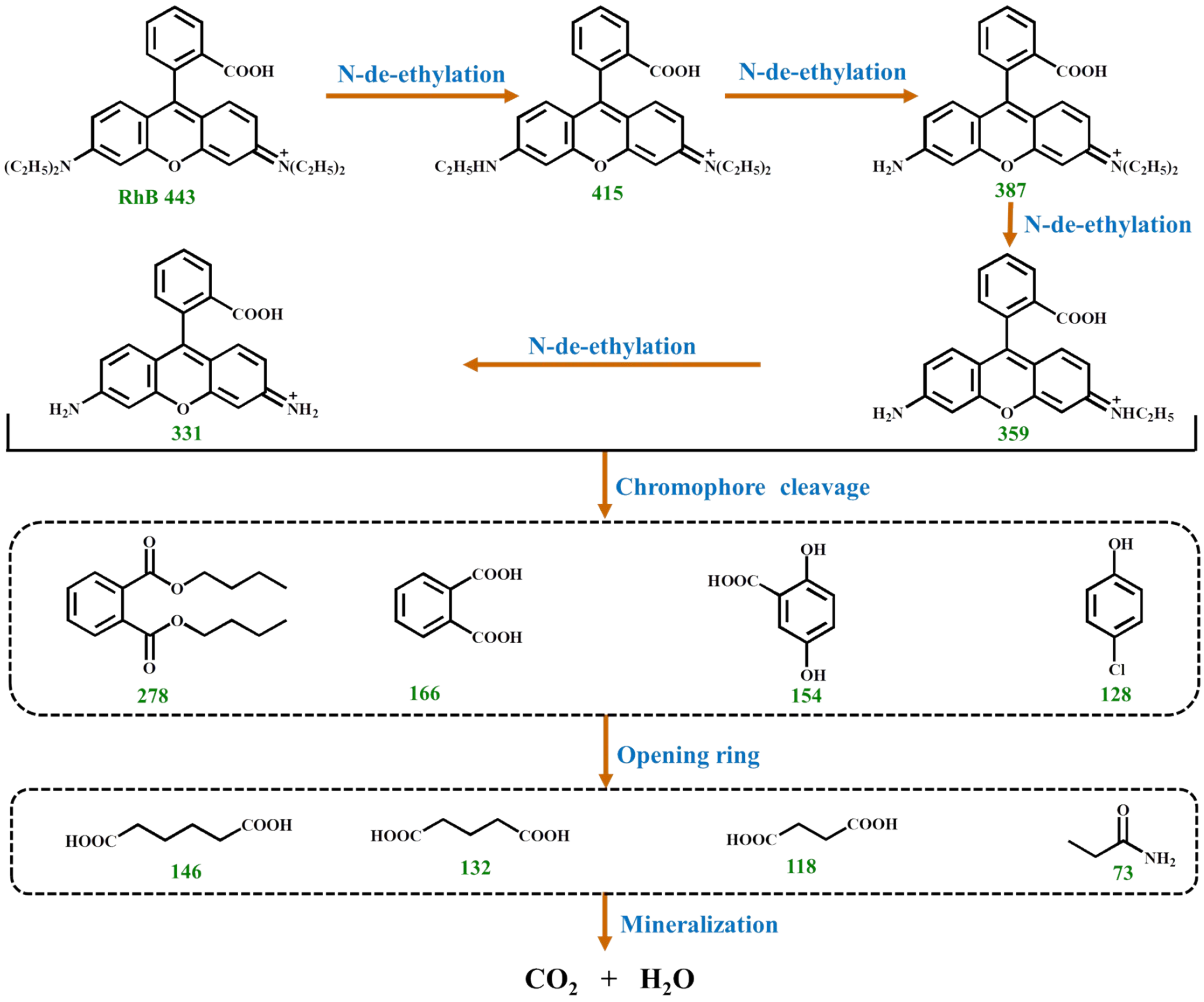

Fig. S19. Possible radical degradation pathway of RhB in Fe^0/PMS system.

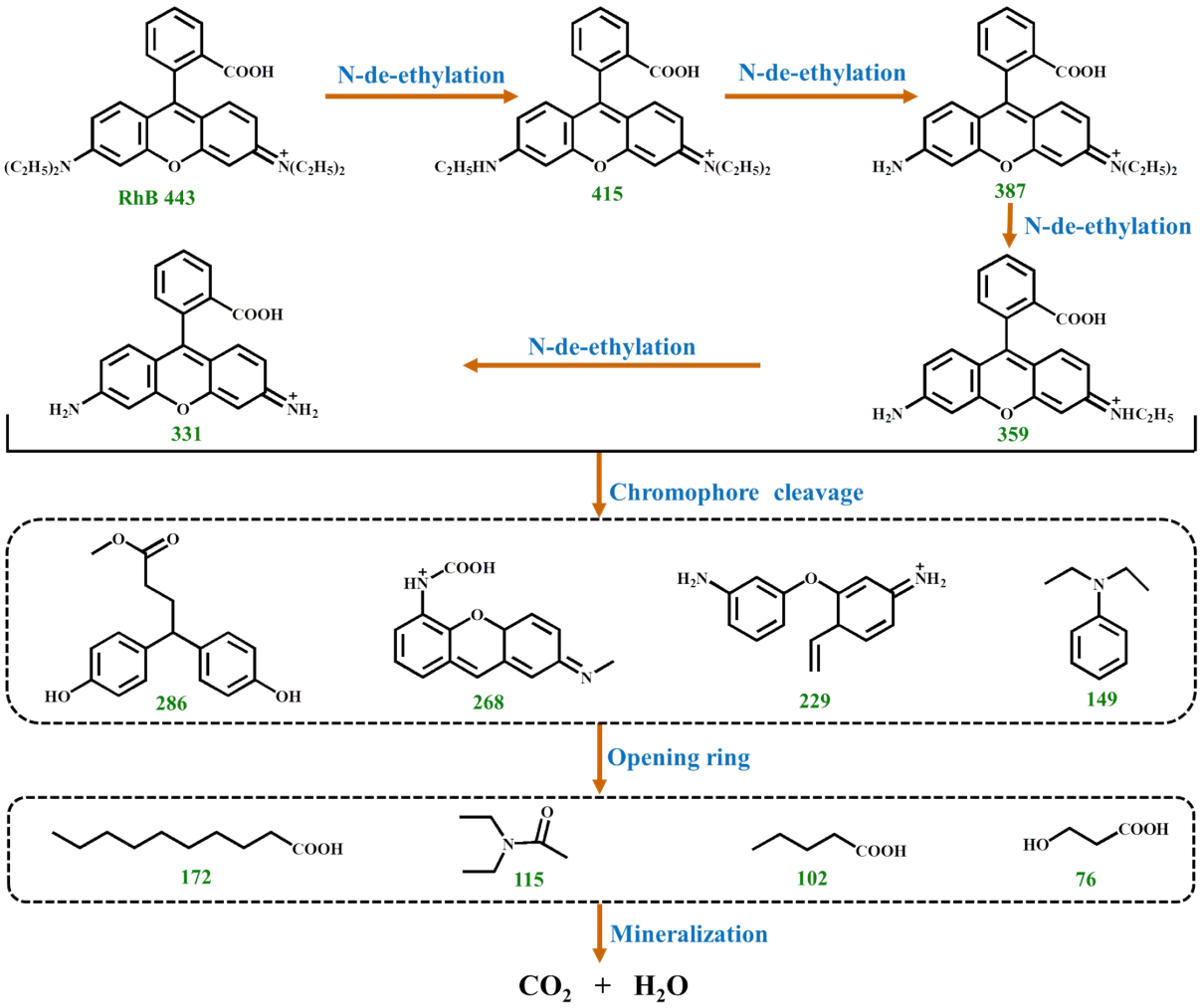

Fig. S20. Possible nonradical degradation pathway of RhB in GNG/PMS system.

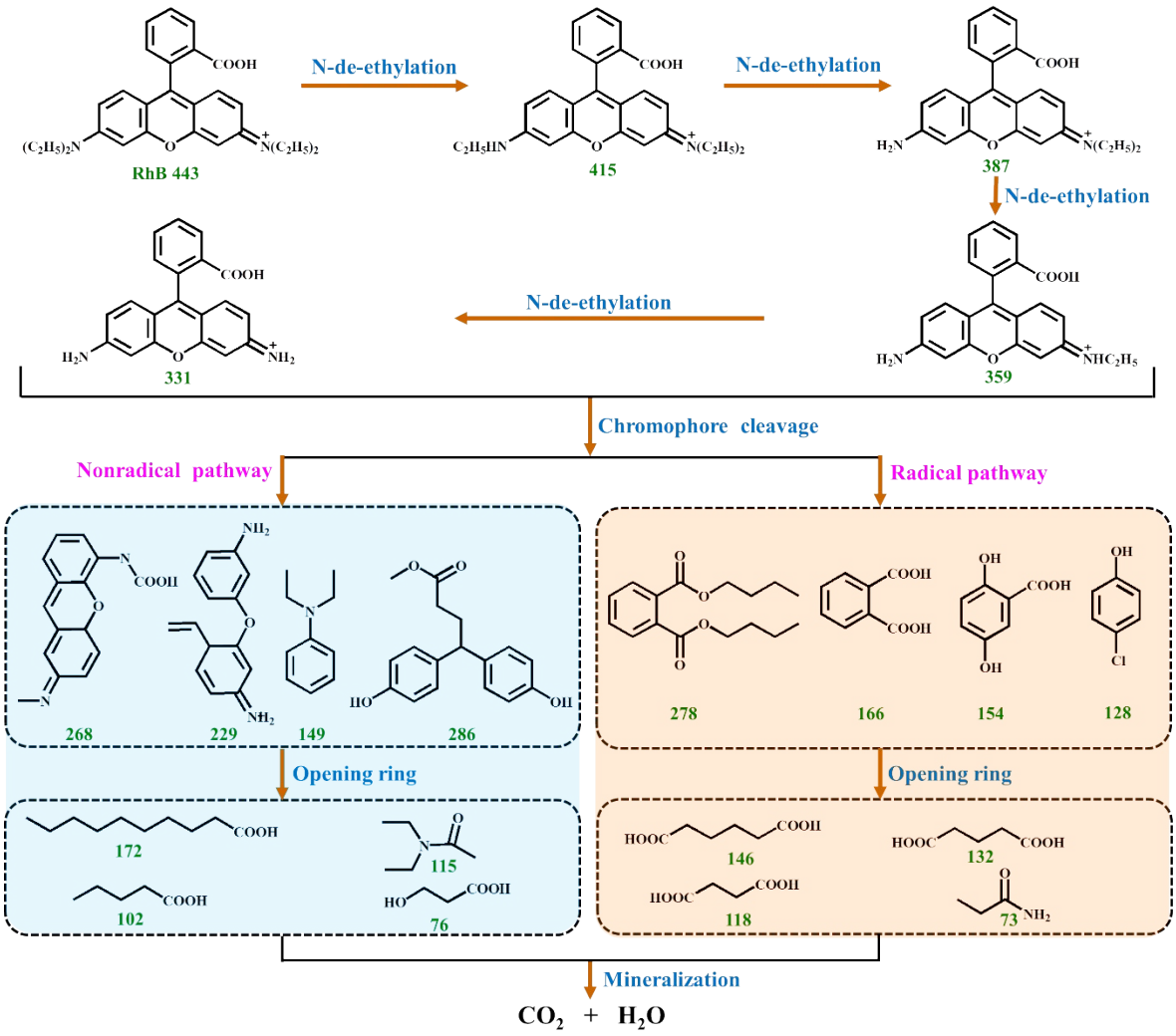

Fig. S21. Proposed degradation pathways of RhB in Fe-GNG2/PMS system.

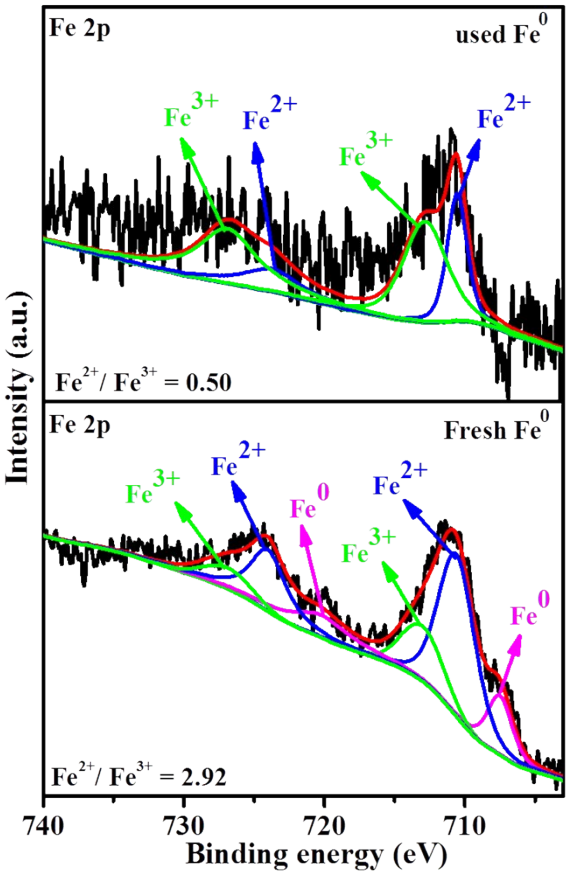

Fig. S22. Fe 2p XPS spectra of fresh and used Fe^0 samples.

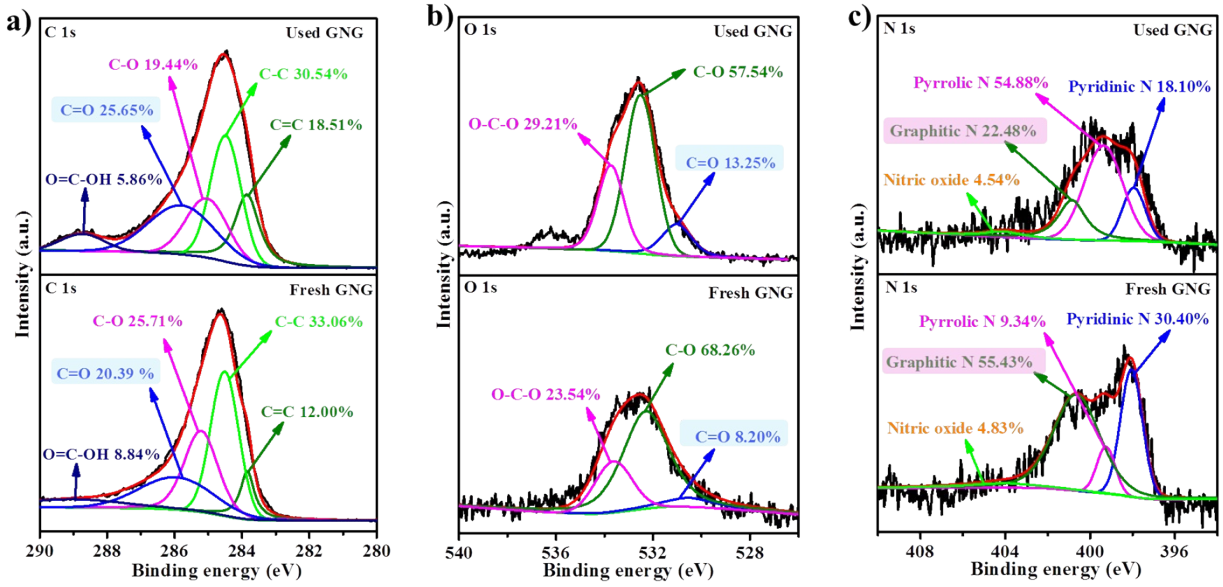

Fig. S23. a) C1s, b) O 1s and c) N1s XPS spectra of fresh and used GNG samples.

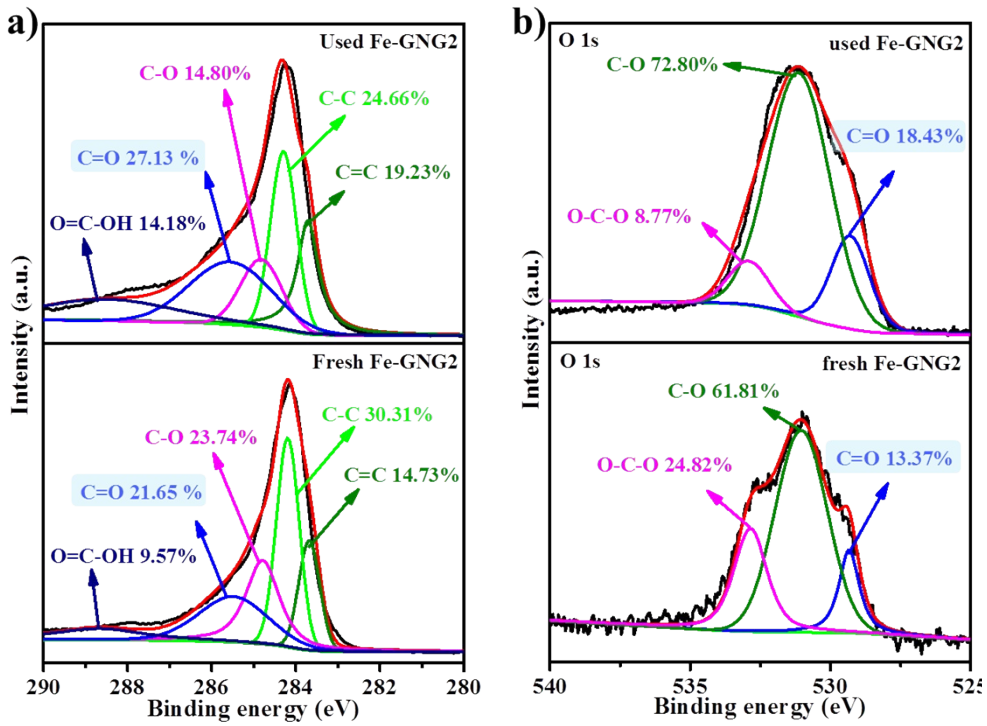

Fig. S24. a) C1s and b) O 1s XPS spectra of fresh and used Fe-GNG2 samples.

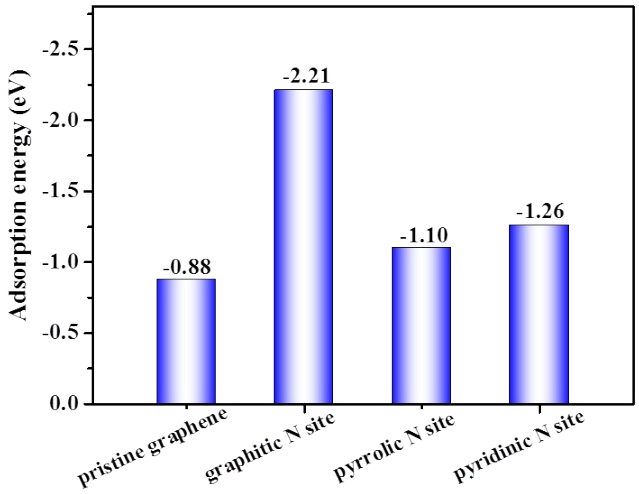

Fig. S25. Adsorption energies of PMS molecule on different sites based on DFT calculations.

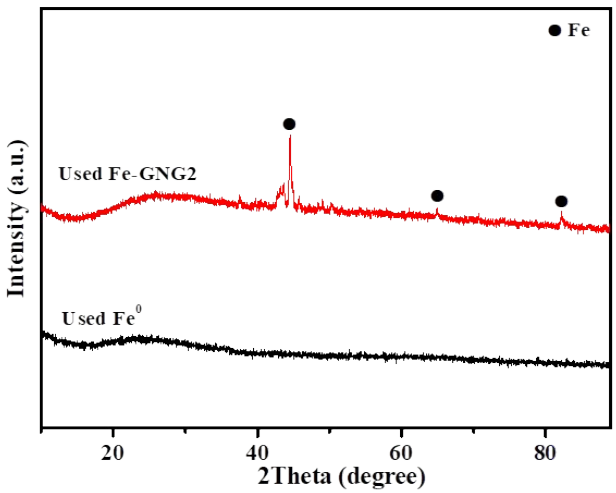

Fig. S26. XRD patterns of used Fe^0 and Fe-GNG2 samples.

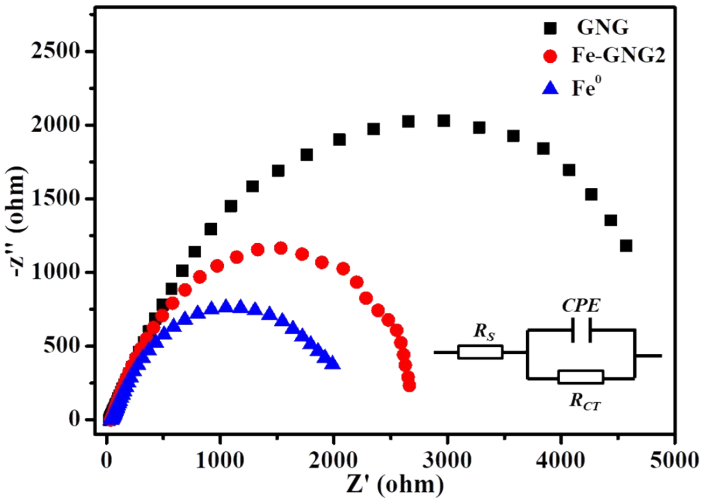

Fig. 27. EIS Nyquist plots of Fe^0, GNG and Fe-GNG2 samples.

Table S1 RhB degradation performance by different catalysts.

Catalyst	RhB concentration (mg/L)	Catalyst amount (mg/L)	PMS amount (mM)	Reaction time (min)	Remove rate (%)	Activation energy (kJ/mol)	Ref.
Fe-GNG2	20	25	0.10	70	100	5.28	This work
Porous Fe_2O_3	50	1500	1	60	100	69.23	5
CoMg/SBA-15	5	250	0.2	120	100	/	6
5%Ca-Fe_2O_3	10	500	0.3	120	99	/	7
$ZnFe_{0.8}Co_{0.4}O_{2.4}$	10	200	0.1	14	100	/	8
Si–N/C	20	200	2	7	100	/	9
$CoMn_2O_4$/HACNFs	24	20	1	60	100	36.06	10
Cu/ZSM5	25	1000	1	15	100	/	11
rGO-CoPc	12	500	0.1	15	100	/	12
FeCo-LDH	20	200	0.2	10	100	59.71	13
MCCI	10	50	0.8	30	80	38.70	14
Co_2SnO_4	12	500	0.1	16	60	/	15
Fe/Co-N/P-9	40	60	0.65	35	98	/	16
CuO-CeO_2	48	400	1.6	60	100	/	17
Co-HAP-2	40	200	0.4	12	93	/	18
Fe-Co-Co PBA@PmPDs	15	100	0.5	60	99.7	98.31	19
ZVI	20	100	0.4	60	100	/	20
CZIF-67@SiO_2	50	40	0.4	30	100	/	21
[#]Ag-$ZnFe_2O_4$@rGO	10	500	/	30	95.5	/	22
[#]FeCit@ACFs	24	2000	4	33	82.2	/	23
[#]C1B2O-5	24	800	0.65	180	100	/	24

[#] under light irradiation.

Table S2 CTC degradation performance by different catalysts.

Catalyst	CTC concentration (mg/L)	Catalyst amount (mg/L)	PMS amount (mM)	Reaction time (min)	Remove rate (%)	Ref.
Fe-GNG2	20	25	0.10	60	100	This work
Co@NC-800	30	200	0.33	30	90	25
R-NAu-2	48	2000	2	5	75	26
5CN-CG	30	1000	0.81	30	88	27
#re-Mn-CeO_2	14	100	0.3	30	100	28
#FCN-12	30	600	0.65	120	83.4	29
#Er-Fe-TiO_2-dcbpy	10	50	/	60	99.8	30
#PDI	20	500	/	150	< 70	31
#GO/PAA-CdS	30	150	/	240	85	32

under light irradiation.

Table S3 ANOVA results regarding the effects of experimental parameters on RhB and CTC removal.

Parameter	RhB removal				CTC removal			
	df	SS	F	P	df	SS	F	P
Fe-GNG dosage	3	0.07	101	< 0.0001	3	0.30	455	< 0.0001
PMS dosage	3	1.02	1993	< 0.0001	3	0.72	2080	< 0.0001
Temperature	2	0.00	1.01	0.4202	2	0.00	0.58	0.5869
Initial solution pH	4	0.10	99.0798	< 0.0001	/	/	/	/

Table S4 Fe^{2+}/Fe^{3+} ratios of Fe^0 and Fe-GNG2 before and after use from XPS analyses.

Sample	Fe^{2+}/Fe^{3+}
Fresh Fe^0	2.92
Used Fe^0	0.50
Fresh Fe-GNG2	2.94
Used Fe-GNG2	2.20

Table S5 Proportions of different C groups of GNG and Fe-GNG2 before and after use from XPS analyses.

Sample	O=C-OH/C_{total} %	C=O/C_{total} %	C-O/C_{total} %	C-C/C_{total} %	C=C/C_{total} %
Fresh GNG	8.84	20.39	25.71	33.06	12.00
Used GNG	5.86	25.65	19.44	30.54	18.51
Fresh Fe-GNG2	9.57	21.65	23.74	30.31	14.73
Used Fe-GNG2	14.18	27.13	14.80	24.66	19.23

Table S6 Proportions of different O groups of GNG and Fe-GNG2 before and after use from XPS analyses.

Sample	O-C-O/O_{total} %	C-O/O_{total} %	C=O/O_{total} %
Fresh GNG	23.54	68.26	8.20
Used GNG	29.21	57.54	13.25
Fresh Fe-GNG2	24.82	61.81	13.37
Used Fe-GNG2	8.77	72.80	18.43

Table S7 Proportions of different N groups of GNG and Fe-GNG2 before and after use from XPS analyses.

Sample	$N_{pyridinic}/N_{total}$ %	$N_{pyrrolic}/N_{total}$ %	$N_{graphitic}/N_{total}$ %	$N_{nitric\ oxide}/N_{total}$ %
Fresh GNG	30.40	9.34	55.43	4.83
Used GNG	18.10	54.88	22.48	4.54
Fresh Fe-GNG2	34.96	4.40	59.30	1.30
Used Fe-GNG2	12.63	46.19	34.05	7.13

Table S8 Water quality of tap water.

No.	Substance	Concentration
1	ammonia nitrogen	< 0.02 mg/L
2	cyanogen chloride	< 0.01 mg/L
3	atrazine	< 0.0001 mg/L
4	1.2-dichlorobenzene	< 0.001 mg/L
5	chlorobenzene	< 0.001 mg/L
6	parathion	< 0.001 mg/L
7	2,4,6-trichlorophenol	< 0.0005 mg/L
8	α-1,2,3,4,5,6-hexachlorocyclohexane	≤ 0.000002 μg/L

[#] The data came from Wuhan Water Affairs Group Co., Ltd. (http://www.whwater.com/gsfw/szgg).

Table S9 Water qualities of East Lake water and Yangtze River water.

No.	Substance	Concentration
1	nitrate	≤ 20 mg/L
2	nitrite	≤ 0.02 mg/L
3	sulfate	≤ 250 mg/L
4	chloride	≤ 250 mg/L
5	Fe ion	≤ 0.3 mg/L
6	Co ion	≤ 0.05 mg/L
7	cyanide	≤ 0.05 mg/L
8	volatile phenols	≤ 0.002 mg/L
9	anionic synthetic detergent	≤ 0.3 mg/L
10	α-1,2,3,4,5,6-hexachlorocyclohexane	≤ 5.0 μg/L
11	dichlorodiphenyltrichloroethane	≤ 1.0 μg/L

[#] The data came from Wuhan Environmental Protection Bureau (http://hbj.wuhan.gov.cn/hjsj/).

References

1. J. Zhang, P. Chen, W. Gao, W. Wang, F. Tan, X. Wang, X. Qiao and P. K. Wong, *Sep. Purif. Technol.*, 2021, **265**, 118474.
2. G. Kresse and J. Hafner, *Phys. Rev. B*, 1994, **49**, 14251-14269.
3. S. Grimme, J. Antony, S. Ehrlich and H. Krieg, *J. Chem. Phys.*, 2010, **132**, 154104-154123.
4. G. Kresse and D. Joubert, *Phys. Rev. B*, 1991, **59**, 1758-1775.
5. F. Ji, C. Li, X. Wei and J. Yu, *Chem. Eng. J.*, 2013, **231**, 434-440.
6. L. Hu, F. Yang, W. Lu, Y. Hao and H. Yuan, *Appl. Catal. B: Environ.*, 2013, **134-135**, 7-18.
7. S. Guo, H. Wang, W. Yang, H. Fida, L. You and K. Zhou, *Appl. Catal. B: Environ.*, 2020, **262**, 118250-118262.
8. H. Zhang, C. Li, L. Lyu and C. Hu, *Appl. Catal. B: Environ.*, 2020, **270**, 118874.
9. W. Duan, J. He, Z. Wei, Z. Dai and C. Feng, *Environ. Sci.: Nano*, 2020, **7**, 2982-2994.
10. S. Kang and J. Hwang, *Chem. Eng. J.*, 2021, **406**, 127158.
11. F. Ji, C. Li, Y. Liu and P. Liu, *Sep. Purif. Technol.*, 2014, **135**, 1-6.
12. M. Cornelia, B. A. Monaam, H. Abderrahmane, C. Yacine, B. Alexandre, C. Yannick, S. Simona, R. Valentin, S. Sabine and B. Rabah, *Chem. Eng. J.*, 2018, **336**, 465-475.
13. C. Gong, F. Chen, Q. Yang, K. Luo, F. Yao, S. Wang, X. Wang, J. Wu, X. Li, D. Wang and G. Zeng, *Chem. Eng. J.*, 2017, **321**, 222-232.
14. A. Lin and B. Chen, *Chemosphere*, 2017, **166**, 146-156.
15. M. B. Ali, A. Barras, A. Addad, B. Sieber, H. Elhouichet, M. Ferid, S. Szunerits and R. Boukherroub, *Phys Chem Chem Phys*, 2017, **19**, 6569-6578.

16. L. Wang, J. Di, J. Nie and G. Ma, *ACS Appl. Nano Mater.*, 2019, **2**, 6998-7007.

17. Z. Li, D. Liu, Y. Zhao, S. Li, X. Wei, F. Meng, W. Huang and Z. Lei, *Chemosphere*, 2019, **233**, 549-558.

18. Y. Pang, L. Kong, D. Chen, G. Yuvaraja and S. Mehmood, *J. Hazard. Mater.*, 2020, **384**, 121447-121458.

19. L. Zeng, L. Xiao, X. Shi, M. Wei, J. Cao and Y. Long, *J. Colloid Interface Sci.* , 2019, **534**, 586-594.

20. X. Ding, L. Gutierrez, J. P. Croue, M. Li, L. Wang and Y. Wang, *Chemosphere*, 2020, **253**, 126655.

21. W. Li, Y. Zhang, P. Zhao, P. Zhou, Y. Liu, X. Cheng, J. Wang, B. Yang and H. Guo, *J. Hazard. Mater.*, 2020, **393**, 122399-122409.

22. A. H. Mady, M. L. Baynosa, D. Tuma and J. J. Shim, *Appl.Catal. B: Environ.*, 2017, **203**, 416-427.

23. L. Luo, D. Wu, D. Dai, Z. Yang, L. Chen, Q. Liu, J. He and Y. Yao, *Appl. Catal. B: Environ.*, 2017, **205**, 404-411.

24. Y. Wang, C. Liu, Y. Zhang, W. Meng, B. Yu, S. Pu, D. Yuan, F. Qi, B. Xu and W. Chu, *Appl. Catal. B: Environ.*, 2018, **235**, 264-273.

25. J. Cao, Z. Yang, W. Xiong, Y. Zhou, Y. Wu, M. Jia, S. Sun, C. Zhou, Y. Zhang and R. Zhong, *Sep. Purif. Technol.*, 2020, **250**, 117237.

26. N. Chen, G. Fang, C. Zhu, S. Wu, G. Liu, D. D. Dionysiou, X. Wang, J. Gao and D. Zhou, *J. Hazard. Mater.*, 2020, **389**, 121819.

27. X. Zhang, R. Zhao, N. Zhang, Y. Su, Z. Liu, R. Gao and C. Du, *Appl. Catal. B : Environ.*,

2020, **263**, 118316.

28. A. Wang, Z. Zheng, H. Wang, Y. Chen, C. Luo, D. Liang, B. Hu, R. Qiu and K. Yan, *Appl. Catal. B : Environ.*, 2020, **277**, 119171.
29. H. Guo, H. Niu, C.Liang, C. Niu, Y. Liu, N. Tang, Y. Yang, H. Liu, Y. Yang and W. Wang, *Chem. Eng. J.*, 2020, **401**, 126072.
30. L. Wang, Y. Chen, Y. Zheng, X. Cheng, J. Hao and Q. Shang, *Chem. Eng. J.*, 2021, **410** 128319.
31. Q. Zhang, L.Jiang, J.Wang, Y. Zhu, Y. Pu and W. Dai, *Appl. Catal. B : Environ.*, 2020, **277**, 119122.
32. W. Kong, Y.Gao, Q. Yuea, Q. Li, B. Gao, Y. Kong, X. Wang, P. Zhang and Y. Wang, *J. Hazard. Mater.*, 2020, **388** 121780.